Experimental Demonstration of the Widely Linear Sparse Volterra Equalizer Used in Probabilistic Shaping 1024-QAM Transmission with Spectral Efficiency of 16.57-bit/s/Hz

Nan Wang
State Key Laboratory of Information Photonics and Optical Communications
Beijing University of Posts and Telecommunications (BUPT)
Beijing, China
wangnann@bupt.edu.cn

Feng Tian
State Key Laboratory of Information Photonics and Optical Communications
Beijing University of Posts and Telecommunications (BUPT)
Beijing, China
tianfeng@bupt.edu.cn

Tianze Wu
State Key Laboratory of Information Photonics and Optical Communications
Beijing University of Posts and Telecommunications (BUPT)
Beijing, China
wutianze@bupt.edu.cn

Xiangjun Xin
State Key Laboratory of Information Photonics and Optical Communications
Beijing University of Posts and Telecommunications (BUPT)
Beijing, China
xjxin@bupt.edu.cn

Bo Liu
Institute of Optics and Electronics
Nanjing University of Information Science & Technology (NUIST)
Nanjing, China
bo@bupt.edu.cn

Qi Zhang
State Key Laboratory of Information Photonics and Optical Communications
Beijing University of Posts and Telecommunications (BUPT)
Beijing, China
zhangqi@bupt.edu.cn

Wei Gao
Artificial Intelligence Center
Changzhou Jingxin New Generation Information Technology Research Institute
Changzhou, China
gaowei@ngiic.com

***Abstract*—The widely linear sparse Volterra equalizer is proposed in this paper, and the performance is demonstrated in the polarization multiplexed probabilistic shaping 1024-QAM with the spectral efficiency of 16.57-bit/s/Hz.**

Keywords—Complex-valued widely linear equalizer, high spectral efficiency, multi-input multi-output Volterra equalizer, ultra-high-order modulation.

I. INTRODUCTION

With the development of information science and 5G networks, the demand for information acquisition and exchange is growing rapidly [1-2]. Ultra high-order quadrature amplitude modulation (QAM) is becoming the focus of the communication industry because of its high spectral efficiency [3-5]. Ultra high-order QAM signals are known to be challenging to generate and recover. Limitations form hardware such as quantization noise, isotropic quadrature modulator imbalance, bandwidth limitations of digital-to-analog/analog-to-digital converters, and laser linewidth [6-7].

In this paper, we focus on the polarization-multiplexed probabilistically shaped (PM-PS) 1024-QAM format and provide a feasible scheme for PM-PS-1024-QAM signals based on offline DSP, and utilize a 2×2 MIMO widely linear complex-valued sparse Volterra (MIMO-WLCSV) equalizer based on the recursive least square (RLS) error, which consists of a 1st-order 2×2 MIMO complex valued widely linear equalizer and a 3rd-order real-valued linear equalizer. The proposed MIMO-WLCSV can effectively compensate for IQ imbalances and nonlinear impairments induced by the device [8-11]. Sparseness is also utilized to reduce the complexity [12]. In this paper, the experimental results show spectral efficiency can reach 16.57 bit/s/Hz, and the BER can reach 6.11×10^{-4} using PM-PS-1024-QAM signals.

II. PRINCIPLE OF THE ALGORITHM

The structure diagram of the general complex-valued 2×2 MIMO equalizer is shown in Fig. 1 and can be presented mathematically by (1),

$$\begin{bmatrix} x_{out} \\ y_{out} \end{bmatrix} = \begin{bmatrix} w_{xx} & w_{xy} \\ w_{yx} & w_{yy} \end{bmatrix} \begin{bmatrix} x_{in} \\ y_{in} \end{bmatrix} \tag{1}$$

where w denotes the weight of the equalizer taps, x_{in} and y_{in} are the inputs of the equalizer, and x_{out} and y_{out} are the outputs of the equalizer. Four *Nth*-order real coefficient number filters typically need to implement the *Nth*-order complex filter. For the 2×2 MIMO complex-valued equalizer mentioned in Fig. 1, it is implemented by four 2×2 real-valued equalizers.

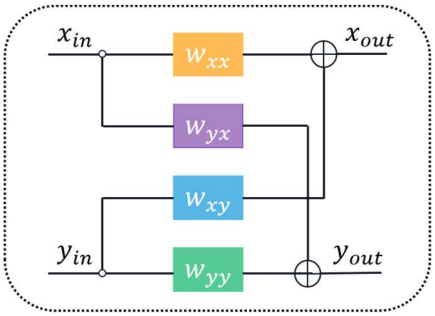

Fig. 1. Structure diagrams of 2×2 MIMO complex-valued equalizer.

As the device characteristics of the two I/Q branches are not perfectly matched, for example, the I/Q features of the LO, the frequency response of the respective low-pass filters of the I/Q branches are not perfectly matched, causing the IQ imbalance. In addition, electrical amplifiers, AWG output RF lines, MZM modulators, and balanced detectors generally

cause nonlinear impairment, especially in ultra-high-order QAM. Considering that a complex-valued equalizer can overcome the IQ imbalance and a Volterra equalizer can simultaneously compensate for linear and nonlinear impairments. We utilized a 2×2 MIMO-WLCSV equalizer. The structure of MIMO-WLCSV is illustrated in Fig. 2, which can be represented as given below by (2):

$$\begin{bmatrix} x_{out} \\ y_{out} \end{bmatrix} = \begin{bmatrix} w_{xx} & w_{xy} \\ w_{yx} & w_{yy} \end{bmatrix} \begin{bmatrix} x_{in} \\ y_{in} \end{bmatrix} + \begin{bmatrix} w_{xx}^* & w_{xy}^* \\ w_{yx}^* & w_{yy}^* \end{bmatrix} \begin{bmatrix} x_{in}^* \\ y_{in}^* \end{bmatrix} + \begin{bmatrix} w_{xr2} & w_{xi2} \\ w_{yr2} & w_{yi2} \end{bmatrix} \begin{bmatrix} x_{in2} \\ y_{in2} \end{bmatrix} + \begin{bmatrix} w_{xr3} & w_{xi3} \\ w_{yr3} & w_{yi3} \end{bmatrix} \begin{bmatrix} x_{in3} \\ y_{in3} \end{bmatrix} \quad (2)$$

where $[\cdot]^*$ means complex conjugate, w_{xi} is the weight of *ith*-order equalizer taps. x_{in2} and x_{in3} mean inputs of the 2nd-order and 3rd-order kernel.

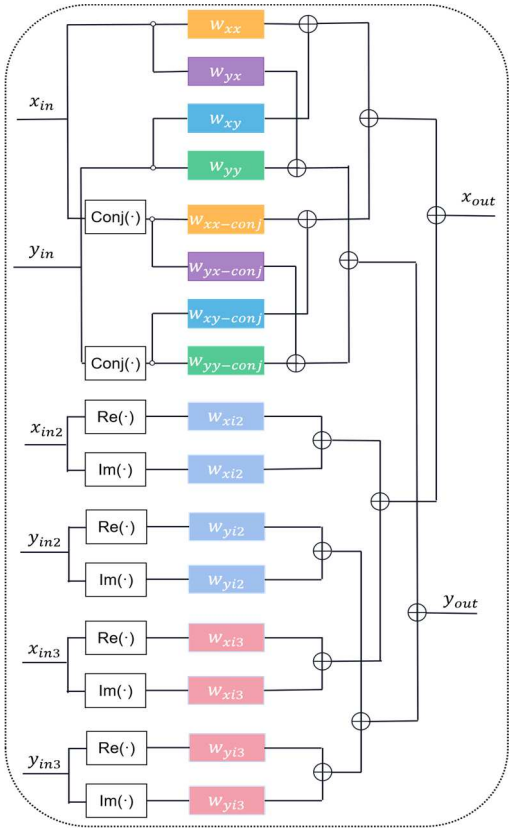

Fig. 2. Structure diagrams of the proposed MIMO-WLCSV.

In addition to the Volterra series, we know the complexity mainly comes from the 2nd-order and 3rd-order kernels. We utilize a sparse method based on the l_0 norm to reduce the complexity. Defined kth-order normalized kernel weights are the ratio of the *kth*-order weights to the *kth*-order maximum weights, which means the smaller normalized weights are less critical and have less impact on the system equilibrium performance. By selecting the minimum threshold of normalized weight and deleting all taps below the threshold point, the updated equation for RLS weights can be given as:

$$w(k+1) = w(k) + e(k)z(k) - S(k) \quad (3)$$

$$S(k) = \gamma(1-\lambda)P(k)\nabla^s f\big(w(k-1)\big) \quad (4)$$

where $e(k)$ are the error at the moment k, $S(k)$ are terms for sparse, γ is the regularization parameter, λ is the forgetting factors, $z(k)$ and $P(k)$ are *kth*-order iteration value, $f\left(w(k)\right)$ is the l_0 norm of w(k), $\nabla^s f\left(w(k)\right)$ is the subdifferential of $f\left(w(k)\right)$.

We compare the commonly used real-valued 2×2 MIMO equalizer, based on the RLS and least mean square (LMS) error, respectively. The experimental results verified the proposed MIMO-WLCSV shown below. Furthermore, the number of 1st-order, 2nd-order, and 3rd-order memory lengths are set to 121, 41, and 5 concerning performance and complexity. In the experiments, we mainly focused on 2nd-order kernels. Fig. 3(a) shows the modulus of weights for the first 200 2nd-order kernels after training. Deleting all taps below the threshold, which are marked in red in Fig. 3(b) can reduce the complexity of Volterra equalizer.

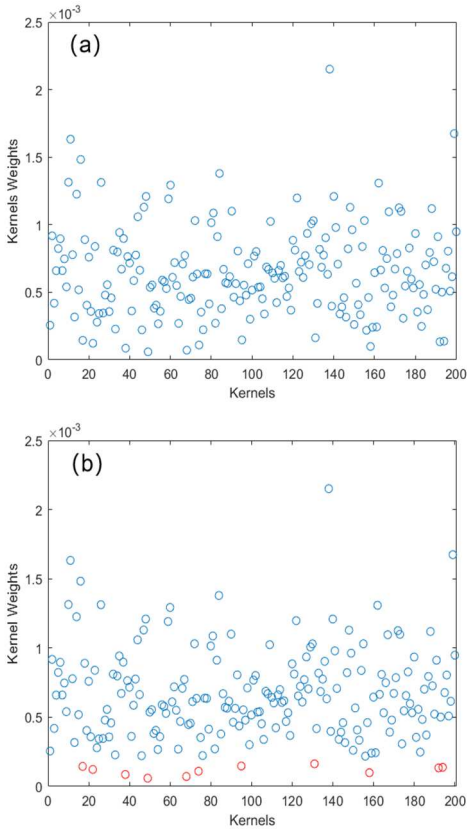

Fig. 3. Principle of sparse Volterra.

The complexity of the system is calculated and can be represented as:

$$C_1 = M_1 + 2M_2 + 3M_3 \quad (5)$$

$$C_2 = M_1 + 2(M_2 - N_2) + 3(M_3 - N_3) \quad (6)$$

where M_1, M_2 and M_3, mean the number of taps of 1st-order, 2nd-order and 3rd-order, N_1 and N_2 mean the number of deleted taps of 2nd-order and 3rd-order. C_1 and C_2 mean the full Volterra complexity and the sparse Volterra complexity. The complexity of the system reduction can be represented as：

$$P = 1 - \frac{C_2}{C_1} \quad (7)$$

III. Experimental Setup

The setup is illustrated in Fig. 4. The PS-1024-QAM signals are generated at the transmitter by a high-precision arbitrary waveform generator (AWG) and passed through an IQ modulator, which mixes the data with an optical carrier. The laser generates light with a linewidth of 1 kHz and a wavelength of 1550 nm, then divided into two paths by a 2×2 coupler. The two light paths are fed to the IQ modulator as the optical carrier and the receiver as the local oscillation source, respectively. Then the modulated light is implemented by the delay line for polarization multiplexing. An EDFA and VOA control the signal-to-noise ratio of the signal. After 10 km of standard single-mode fiber, the signals are received by a homodyne integrated coherent receiver (ICR) with a bandwidth of 20 GHz. Then collected through a digital storage oscilloscope with a 3-dB bandwidth of 20 GHz and a sampling rate of 100-GSa/s and processed by offline DSP.

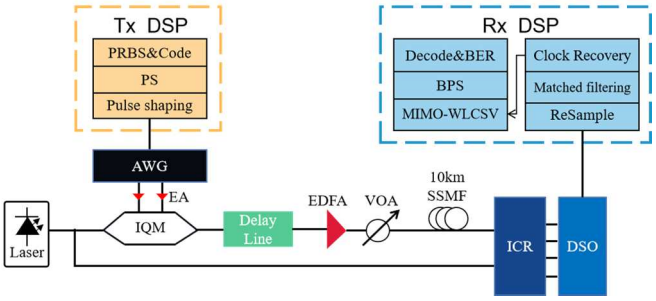

Fig. 4. Experimental setup for PM-PS-1024-QAM system. AWG: arbitrary waveform generator, EA: electric amplifier, IQM: IQ modulator, SSMF: strander single mode fiber, EDFA: Erbium-doped fiber amplifier, VOA: variable low pass filter, ICR: intradyne coherent receiver, DSO: digital storage oscilloscope, MIMO-WLCSVL: MIMO widely linear complex-valued sparse Volterra.

The offline DSP algorithm at the transmitter and receiver sides of the system is illustrated in Fig. 4. At the transmitter side, the pseudo-random binary sequence is encoded with PS-1024-QAM pulse shaping, and the roll-off factor is 0.05. The DSP algorithm includes resampling, matched filtering, clock recovery, MIMO-WLCSV, BPS, and decoding algorithm on the receiver side.

IV. Results And Discussion

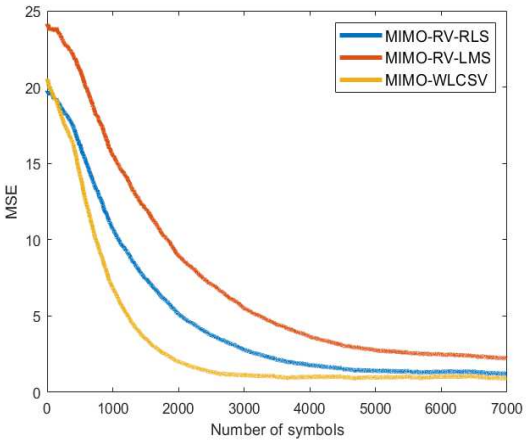

Fig. 5. X polarization MSE versus symbol number for MIMO-RV-RLS, MIMO-RV-LMS, and MIMO-WLCSV.

Fig. 5 illustrates the MSE and symbol number relationship. It can be seen MIMO-WLCSV converges faster and better than the MIMO-RV-LMS and MIMO-RV-RLS equalizer. The experimental results prove that MIMO-WLCSV can effectively deal with the ultra-high-order modulation format's IQ imbalance and nonlinear impairment.

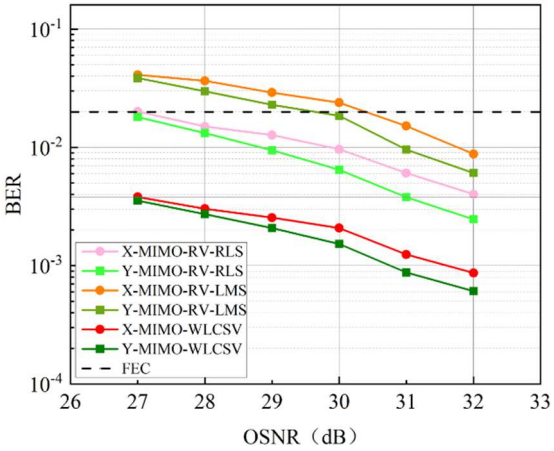

Fig. 6. The relationship of SNR versus BER for PM-PS-1024-QAM.

Fig. 6 illustrates the OSNR versus BER relationship of 1G Baud PS-1024-QAM after 10km fiber. The shaping factor is 0.02 and the spectral efficiency is 16.57 bit/s/Hz. It can be seen that the BER can meet FEC threshold (2×10^{-2}) and the system performance is significantly improved by using MIMO-WLCSV with the same SNR. When the OSNR is 32dB, the system BER reaches 6.11×10^{-4}.

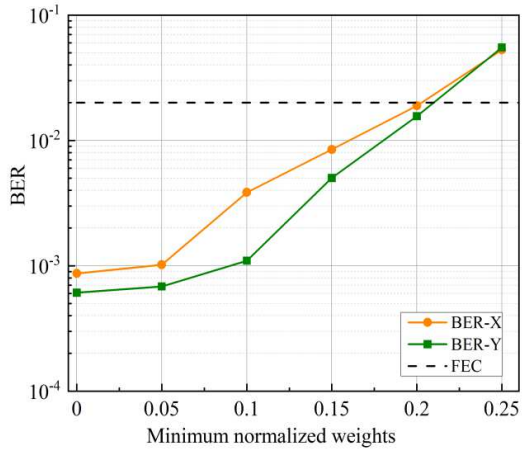

Fig. 7. BER versus minimum normalized weights of 2nd-order Volterra kernels for PM-PS-1024-QAM at 32dB.

Fig. 7 illustrates BER results versus minimum normalized weights of 2nd-order Volterra kernels for PM-PS-1024-QAM at 32dB. The results show that when 2nd-order threshold is 0.2, the BER still meets 2×10^{-2}, at which point the reduced complexity is 8.64%.

V. Conclusion

This paper provides a feasible scheme for PM-PS-1024QAM based on offline DSP. The spectral efficiency achieves 16.57 bit/s/Hz. We utilize a MIMO-WLCSV equalizer compensating the IQ imbalances and nonlinear impairments of the PM-PS-1024-QAM signals. In addition, we introduce sparse based on l_0 norm regularization to reduce the complexity of the Volterra equalizer, which can reduce the algorithm's complexity with less performance loss. The experimental results show that the BER still satisfies the FEC threshold.

ACKNOWLEDGMENT

This work was supported by National Key R&D program of China (2018YFB1800900); National Natural Science Foundation of China (NSFC) (62021005,62027817); Pre-Equipment R&D program of Ministry of Education Joint Foundation (8091B032133); Key R&D program of Changzhou (CE20225005).

REFERENCES

[1] M. Kong et al., "800-Gb/s/carrier WDM Coherent Transmission Over 2000 km Based on Truncated PS-64QAM Utilizing MIMO Volterra Equalizer," in Journal of Lightwave Technology, vol. 40, no. 9, pp. 2830-2839, 1 May1, 2022, Doi: 10.1109/JLT.2022.3148336.

[2] M. Nakamura et al., "Net-bit rate of >562-Gb/s with 32-GBaud Probabilistically Constellation-Shaped 1024QAM Signal Based on Entropy and Code-Rate Optimization," 2022 European Conference on Optical Communication (ECOC), Basel, Switzerland, 2022, pp. 1-4.

[3] J. Ding et al., "High Spectral Efficiency WDM Transmission Based on Hybrid Probabilistically and Geometrically Shaped 256QAM," in Journal of Lightwave Technology, vol. 39, no. 17, pp. 5494-5501, 1 Sept.1, 2021, Doi: 10.1109/JLT.2021.3087919.

[4] J. Ding et al., "Demonstration of 352-Gbit/s Single Line Rate PS-4096QAM THz Wired Transmission over Hollow-Core Fiber," 2021 Opto-Electronics and Communications Conference (OECC), Hong Kong, Hong Kong, 2021, pp. 1-3.

[5] T. Sasai, A. Matsushita, M. Nakamura, S. Okamoto, F. Hamaoka and Y. Kisaka, "Experimental Analysis of Laser Phase Noise Tolerance of Uniform 256QAM and Probabilistically Shaped 1024QAM," 2019 Optical Fiber Communications Conference and Exhibition (OFC), San Diego, CA, USA, 2019, pp. 1-3.

[6] J. Liu, J. Ding, C. Wang, K. Wang, T. Zheng and J. Yu, "8192QAM Signal Transmission by an IM/DD System at W-Band Using Delta-Sigma Modulation," in IEEE Photonics Technology Letters, vol. 35, no. 4, pp. 207-210, 15 Feb.15, 2023, Doi: 10.1109/LPT.2023.3234060.

[7] M. P. Yankov et al., "Constellation Shaping for WDM Systems Using 256QAM/1024QAM With Probabilistic Optimization," in Journal of Lightwave Technology, vol. 34, no. 22, pp. 5146-5156, 15 Nov.15, 2016, Doi: 10.1109/JLT.2016.2607798.

[8] J. Liang, Y. Fan, Z. Tao, X. Su and H. Nakashima, "Transceiver Imbalances Compensation and Monitoring by Receiver DSP," in Journal of Lightwave Technology, vol. 39, no. 17, pp. 5397-5404, 1 Sept.1, 2021, Doi: 10.1109/JLT.2019.2944830.

[9] M. Sato, M. Arikawa, H. Noguchi, J. Matsui, J. Abe and E. L. T. de Gabory, "Transceiver Impairment Mitigation by 8×2 Widely Linear MIMO Equalizer with Independent Complex Filtering on IQ Signals," in IEEE Photonics Journal, vol. 14, no. 3, pp. 1-11, June 2022, Art no. 7130911, Doi: 10.1109/JPHOT.2022.3173652.

[10] A. Frunză, V. Choqueuse, P. Morel and S. Azou, "A Parametric Network for the Global Compensation of Physical Layer Linear Impairments in Coherent Optical Communications," in IEEE Open Journal of the Communications Society, vol. 3, pp. 1428-1444, 2022, Doi: 10.1109/OJCOMS.2022.3201130.

[11] M. B. Salman and G. M. Guvensen, "An Efficient QAM Detector via Nonlinear Post-Distortion Based on FDE Bank Under PA Impairments," in IEEE Transactions on Communications, vol. 69, no. 10, pp. 7108-7120, Oct. 2021, doi: 10.1109/TCOMM.2021.3095974.

[12] Q. Yu et al., "Secure 100 Gb/s IMDD Transmission Over 100 km SSMF Enabled by Quantum Noise Stream Cipher and Sparse RLS-Volterra Equalizer," in IEEE Access, vol. 8, pp. 63585-63594, 2020, doi: 10.1109/ACCESS.2020.2984330.